

## **ANALYSIS ON MHD FLOW OF VISCO-ELASTIC FLUID OF THE TYPE WALTERS LIQUID BAND HEAT TRANSFER OVER A NON-ISOTHERMAL STRETCHING SHEET WITH HOMOTOPY ANALYSIS METHOD**

**<sup>a</sup>M. Hosseini, <sup>b</sup>D. D. Ganji, <sup>\*b</sup>M. Abdollahzadeh, <sup>b</sup>B. SalimBahrami, <sup>b</sup>M. Valizadeh, <sup>b</sup>A. Abbasi & <sup>b</sup>S. Bishehsari**

<sup>a</sup>Dept. of Mechanical Engg., Islamic Azad University, Qhemshahr Branch, P. O. Box 163, Qhaemshahr, Iran

<sup>b</sup>Babol University of Technology, Dept. of Mechanical Engg., P. O. Box 484, Babol, Iran

---

Received: 06th May 2017, Accepted: 12th August 2017

**Abstract:** An analysis has been carried out to study the steady MHD flow and heat transfer in a visco-elastic fluid flow over a semi-infinite, impermeable, non-isothermal stretching sheet with internal heat generation/absorption by the presence of radiation. Thermal conductivity is assumed to vary linearly with temperature. The governing partial differential equations are converted into ordinary differential equations by a similarity transformation. These equations are solved by homotopy analysis method. The effects of different parameters on temperature and velocity profiles are studied. The temperature profiles are shown graphically for different physical parameters.

**Keywords:** Homotopy analysis method, Stretching sheet, Visco-elastic fluid, Heat transfer, Magnetohydrodynamics, Walters liquid B.

### **1. INTRODUCTION**

The study of two-dimensional boundary layer flow over a stretching sheet has gained much interest in recent times because of its numerous industrial applications viz in the polymer processing of a chemical engineering plant and in metallurgy for the metal processing. Crane [1] was first to formulate this problem to study a steady two-dimensional boundary layer flow caused by stretching of a sheet that moves in its plane with a velocity which varies linearly with the distance from a fixed point on the sheet. Many investigators have extended the work of Crane [1] to study heat and mass transfer under different physical situations (e.g., Gupta and Gupta [2], Chen and Char [3], Datta *et al.*, [4], McLeod and Rajagopal [5], Chaim [6, 7]) by including quadratic and higher order stretching velocity. All these works are restricted to Newtonian fluid flows which have received much attention in the last three decades due to their occurrence in nature and their increasing importance in industry. Different types of non-Newtonian fluids are visco-elastic fluid, couple stress fluid, micro polar fluid and power-law fluid. Rajagopal *et al.*, [8] and Siddappa and Abel [9] studied the flow of a visco-elastic fluid flow over a stretching sheet. Troy *et al.*, [10],

---

\* Corresponding Author: [mm.abdollahzadeh@yahoo.com](mailto:mm.abdollahzadeh@yahoo.com)

Wen-Dong [11], Sam Lawrence and Rao [12], McLeod and Rajagopal [5] have discussed the problem of uniqueness/non-uniqueness of the flow of a non-Newtonian visco-elastic fluid over a stretching sheet. Abel and Veena [13] studied the heat transfer of a visco-elastic fluid over a stretching sheet. Bujurke *et al.*, [14] have investigated the heat transfer phenomena in a second order fluid flow over a stretching sheet with internal heat generation and viscous dissipation. Prasad *et al.*, [15] analyzed the problem of a visco-elastic fluid flow and heat transfer in a porous medium over a non-isothermal stretching sheet with variable thermal conductivity. Prasad *et al.*, [16] have investigated on the diffusion of a chemically reactive species of a non-Newtonian fluid immersed in a porous medium over a stretching sheet.

In recent years, the study of MHD flow and heat transfer problems has gained considerable interest because of its extensive engineering applications and may find its applications in polymer technology related to the stretching of plastic sheets. Also, many metallurgical processes involve the cooling of continuous strips or filaments by drawing them through a quiescent fluid and while drawing these strips are sometimes stretched. The rate of cooling can be controlled by drawing such strips in an electrically conducting fluid subjected to a magnetic field in order to get the final products of desired characteristics as the final product greatly depend on the rate of cooling. In view of this, the study of MHD flow of Newtonian/non-Newtonian flow over a stretching sheet was carried out by many researchers (Sarpakaya [17], Pavlov [18], Chakrabarti and Gupta [19], Char [20], Andersson [21], Datti *et al.*, [22], Liao [34-37]).

In the present paper, we study the effect of variable thermal conductivity on the heat transfer of a non-Newtonian visco-elastic fluid of the type Walters Liquid *B*, where thermal conductivity is a function of temperature, subjected to a magnetic field, over a non-isothermal stretching sheet with internal heat generation /absorption. We have assumed that the thermal conductivity is a linear function of the temperature. Further, we consider two cases of non-isothermal boundary conditions namely,

- Surface with prescribed surface temperature (PST Case) and
- Surface with prescribed wall heat flux (PHF Case).

The momentum and energy equations are highly non-linear, and coupled form of partial differential equations (PDEs). These PDEs are then converted to couple non-linear ordinary differential equations (ODEs) by using the similarity variables along with the appropriate boundary conditions. In this paper, we propose to solve these ordinary differential equations analytically by homotopy analysis method [34-37]. Computations are carried out for temperature profiles, Nusselt number when the walls are maintained with prescribed surface temperature and prescribed wall heat flux. Emphasis is given to the effect of thermal radiation on the other physical characteristics.

## 2. BASIC IDEA OF HAM

Let us assume the following nonlinear differential equation in form of:

$$N[u(\tau)] = 0, \quad (2.1)$$

where  $N$  is a nonlinear operator,  $\tau$  is an independent variable and  $u(\tau)$  is the solution of equation. We define the function,  $\phi(\tau, p)$  as follows:

$$\lim_{p \rightarrow 0} \phi(\tau, p) = u_0(\tau), \quad (2.2)$$

where,  $p \in [0, 1]$  and  $u_0(\tau)$  is the initial guess which satisfies the initial or boundary conditions and

$$\lim_{p \rightarrow 1} \phi(\tau, p) = u(\tau), \quad (2.3)$$

and by using the generalized homotopy method, Liao's so-called zero-order deformation equation (1) will be:

$$(1 - p)L[\phi(\tau, p) - u_0(\tau)] = p\hbar H(\tau)N[\phi(\tau, p)], \quad (2.4)$$

where  $\hbar$  is the auxiliary parameter which helps us increase the results' convergence,  $H(\tau)$  is the auxiliary function and  $L$  is the linear operator. It should be noted that there is a great freedom to choose the auxiliary parameter  $\hbar$ , the auxiliary function  $H(\tau)$ , the initial guess  $u_0(\tau)$  and the auxiliary linear operator  $L$ . This freedom plays an important role in establishing the keystone of validity and flexibility of HAM as shown in this paper. Thus, when  $p$  increases from 0 to 1 the solution  $\phi(\tau, p)$  changes between the initial guess  $u_0(\tau)$  and the solution  $u(\tau)$ . The Taylor series expansion of  $\phi(\tau, p)$  with respect to  $p$  is:

$$\phi(\tau, p) = u_0(\tau) + \sum_{m=1}^{+\infty} u_m(\tau) p^m \quad (2.5)$$

and

$$u_0^{[m]}(\tau) = \left. \frac{\partial^m \phi(\tau, p)}{\partial p^m} \right|_{p=0}, \quad (2.6)$$

where  $u_0^{[m]}(\tau)$  for brevity is called the  $m$ th order of deformation derivation which reads:

$$u_m(\tau) = \frac{u_0^{[m]}(\tau)}{m!} = \frac{1}{m!} \left. \frac{\partial^m \phi(\tau, p)}{\partial p^m} \right|_{p=0}. \quad (2.7)$$

It's clear that if the auxiliary parameter  $\hbar = -1$  and auxiliary function  $H(\tau) = 1$ , then Eq. (1) will become:

$$(1 - p)L[\phi(\tau, p) - u_0(\tau)] + p(\tau)N[\phi(\tau, p)] = 0. \quad (2.8)$$

This statement is commonly used in HPM procedure. Indeed, in HPM we solve the nonlinear differential equation by separating any Taylor expansion term. Now we define the vector of:

$$\vec{u}_m = \{\vec{u}_1, \vec{u}_2, \vec{u}_3, \dots, \vec{u}_n\}. \quad (2.9)$$

According to the definition in Eq. (2.7), the governing equation and the corresponding initial conditions of  $u_m(\tau)$  can be deduced from zero-order deformation equation (2.1). Differentiating Eq. (2.1)  $m$  times with respect to the embedding parameter  $p$  and setting  $p = 0$  and finally dividing by  $m!$ , we will have the so-called  $m$ th-order deformation equation in the form:

$$L[u_m(\tau) - \chi_m u_{m-1}(\tau)] = \hbar H(\tau)R(\vec{u}_{m-1}), \quad (2.10)$$

where:

$$R_m(\bar{u}_{m-1}) = \frac{1}{(m-1)!} \left. \frac{\partial^{m-1} N[\phi(\tau, p)]}{\partial p^{m-1}} \right|_{p=0}, \quad (2.11)$$

and

$$\chi_m = \begin{cases} 0, & m \leq 1, \\ 1, & m > 1. \end{cases} \quad (2.12)$$

So by applying inverse linear operator to both sides of the linear equation, Eq. (2.1), we can easily solve the equation and compute the generation constant by applying the initial or boundary condition.

### 3. GOVERNING EQUATIONS AND SIMILARITY ANALYSIS

#### 3.1. Flow Analysis

Consider a steady, laminar flow of an incompressible and electrically conducting visco-elastic fluid over a semi-infinite, impermeable stretching sheet (Fig. 1). Two equal and opposite forces are introduced along the  $x$ -axis so that the sheet is stretched with a speed proportional to the distance from the origin. The resulting motion of the otherwise quiescent fluid is thus caused solely by the moving surface. A uniform magnetic field of strength  $B_0$  is imposed along  $y$ -axis.

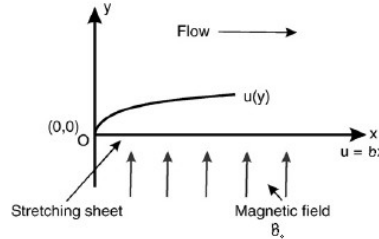


**Figure 1:** Physical Model for Hydromagnetic Stretching Sheet Flow

This flow satisfies the rheological equation of state derived by Beard and Walters [23]. The steady two dimensional boundary layer equations for this flow in usual notation are

$$\frac{\partial u}{\partial x} + \frac{\partial v}{\partial y} = 0, \quad (3.1)$$

$$u \frac{\partial u}{\partial x} + v \frac{\partial u}{\partial y} = \gamma \frac{\partial^2 u}{\partial^2 y^2} - \frac{\sigma B_0^2}{\rho} u - k_0 \left\{ u \frac{\partial^3 u}{\partial x \partial y^2} + v \frac{\partial^3 u}{\partial y^3} + \frac{\partial u}{\partial x} \frac{\partial^2 u}{\partial y^2} - \frac{\partial u}{\partial y} \frac{\partial^2 u}{\partial x y} \right\}. \quad (3.2)$$

In deriving these equations it is assumed, in addition to the usual boundary layer approximations that the contribution due to the normal stress is of the same order of magnitude as the shear stress. Here, it is assumed that the magnetic field is applied in the transverse direction of the sheet and the induced magnetic field is negligible. The boundary conditions applicable to the flow problem are

$$\begin{aligned}
u(x, 0) &= bx, & v(x, 0) &= 0, \\
u(x, y) &\rightarrow 0 & \text{as } y &\rightarrow \infty, \\
u_y(x, y) &\rightarrow 0 & \text{as } y &\rightarrow \infty,
\end{aligned} \tag{3.3}$$

with  $b > 0$ . Here  $x$  and  $y$  are, respectively, the directions along and perpendicular to the sheet,  $u$  and  $v$  are the velocity components along  $x$  and  $y$  directions.  $\rho$ ,  $\gamma$ ,  $B_0$ ,  $\sigma$  and  $k_0$  are, respectively, the density, kinematic viscosity, applied magnetic field, induced magnetic field and coefficient of visco-elasticity. The flow is caused solely by the stretching of the sheet, the free stream velocity being zero. Eqs. (3.1) and (3.2) admit a self-similar solution of the form

$$u = bx f_\eta(\eta), \quad v = -\sqrt{b\gamma} f(\eta), \quad \eta = \sqrt{\frac{b}{\gamma}} y, \tag{3.4}$$

where subscript  $\eta$  denotes the differentiation with respect to  $\eta$ . Clearly  $u$  and  $v$  satisfy Eq. (3.1) identically. Substituting these new variables in Eq. (3.2), we have

$$f'^2 - ff'' - f''' + M_n f' + k_1 \{2ff''' - ff^{iv} - f''^2\} = 0, \tag{3.5}$$

where  $M_n = \frac{\sigma B_0^2}{\rho b}$  is the magnetic parameter,  $k_1 = \frac{k_0 b}{\gamma}$  is the visco-elastic parameter, and prime denotes derivatives with respect to  $\eta$ . Using Eq. (3.4), the boundary conditions become

$$f(\eta) = 0 \quad \text{at } \eta = 0, \tag{3.6a}$$

$$f'(\eta) = 0 \quad \text{at } \eta = 0, \tag{3.6b}$$

$$f'(\eta) \rightarrow 0 \quad \text{at } \eta \rightarrow \infty. \tag{3.6c}$$

It is interesting to note that the Eq. (3.5) has exact analytical solution of the form:

$$f' = e^{-\alpha\eta}, \quad \alpha > 0. \tag{3.7}$$

Satisfying the boundary conditions (3.6), Integration of Eq. (3.7) and using (3.6) gives:

$$f = \frac{1}{\alpha} (1 - e^{-\alpha\eta}), \quad \text{where } \alpha = \sqrt{\frac{(1 + M_n)}{(1 - k_1)}}. \tag{3.8}$$

Therefore the velocity components are:

$$u = bx e^{-\alpha\eta}, \quad v = -\sqrt{b\gamma} \frac{1 - e^{-\alpha\eta}}{\alpha}. \tag{3.9}$$

### 3.2. Heat Transfer Analysis

The energy equation for a fluid with variable thermal conductivity in the presence of internal heat generation/absorption for the two-dimensional flow is given by (Chiam [24]):

$$\rho C_p \left( u \frac{\partial T}{\partial x} + v \frac{\partial T}{\partial y} \right) = k(T) \frac{\partial^2 T}{\partial y^2} + \frac{\partial k(T)}{\partial y} \frac{\partial T}{\partial y} + \dot{q} (T - T_\infty) - \frac{\partial q_r}{\partial y}, \tag{3.10}$$

where  $C_p$  is the specific heat at constant pressure,  $T$  is the temperature of the fluid,  $T_\infty$  is the constant temperature of the fluid far away from the sheet,  $k(T)$  is the temperature-dependent thermal conductivity and  $\dot{q}$  is the volumetric rate of heat generation. We consider the temperature-thermal conductivity relationship of the following form (Chiam [24]):

$$k(T) = k_\infty \left( 1 + \frac{\varepsilon}{\Delta T} (T - T_\infty) \right), \quad (3.11)$$

where  $\Delta T = T_w - T_\infty$ ,  $T_w$  is the sheet temperature,  $\varepsilon = -\frac{k_w - k_\infty}{k_\infty}$  is a small parameter and  $k_\infty$  is the conductivity of the fluid far away from the sheet. By using Rosseland approximation [25] the radiative heat flux is given by

$$q_r = -\frac{4\sigma^*}{3k^*} \frac{\partial T^4}{\partial y}, \quad (3.12)$$

where  $\sigma^*$  and  $k^*$  are, respectively, the Stephan–Boltzmann constant and the mean absorption coefficient. We assume that the differences within the flow are such that  $T^4$  can be expressed as a linear function of temperature. This is accomplished by expanding  $T^4$  in a Taylor series about  $T_\infty$  and neglecting higher order terms, thus

$$T^4 \cong 4T_\infty^3 T - 3T_\infty^4 \Rightarrow q_r = -\frac{16\sigma^* T_\infty^3}{3k^*} \frac{\partial T}{\partial y}. \quad (3.13)$$

Substituting Eq. (3.13) and Eq. (3.11) in Eq. (3.10), we get

$$\begin{aligned} \rho C_p \left( u \frac{\partial T}{\partial x} + v \frac{\partial T}{\partial y} \right) &= k_\infty \left( 1 + \frac{\varepsilon}{\Delta T} (T - T_\infty) \right) \frac{\partial^2 T}{\partial y^2} + k_\infty \left( \frac{\varepsilon}{\Delta T} \frac{\partial T}{\partial y} \right)^2 \\ &+ \dot{q} (T - T_\infty) + \frac{16\sigma^* T_\infty^3}{3k^*} \frac{\partial^2 T}{\partial y^2}. \end{aligned} \quad (3.14)$$

The thermal boundary conditions depend on the type of heating process under consideration. Here, we consider two different heating processes, namely, (I) prescribed surface temperature and (II) prescribed wall heat flux, varying with the distance. The boundary conditions assumed for solving Eq. (3.14) are

$$\left. \begin{aligned} T &= T_w = T_\infty + A \left( \frac{x}{l} \right)^r && \text{(PST Case)} \\ -k \frac{\partial T}{\partial y} &= q_w = D \left( \frac{x}{l} \right)^r && \text{(PHF Case)} \end{aligned} \right\} \text{ at } y=0 \text{ and,} \quad (3.15)$$

$$T \rightarrow T_\infty \quad \text{as} \quad y \rightarrow \infty, \quad (3.16)$$

where  $A$  is a constant and depends on the thermal properties of the liquid,  $r$  is the wall temperature parameter,  $q_w$  is the heat flux on the wall surface,  $l = \sqrt{\frac{\gamma}{b}}$  is chosen as characteristic length and  $D$  is a constant. It is obvious now that

$$\Delta T = T_w - T_\infty = \begin{cases} A \left( \frac{x}{l} \right)^r & PST \text{ Case} \\ \frac{D}{k_\infty} \left( \frac{x}{l} \right)^r \sqrt{\frac{\gamma}{b}} & PHF \text{ Case} \end{cases} \quad (3.17)$$

We now use a dimensionless scaled  $\eta$ -dependent temperature of the form

$$\theta(\eta) = \frac{T - T_\infty}{\Delta T}. \quad (3.18)$$

The imminent advantage of using Eq. (3.15) is that the temperature-dependent thermal conductivity turns out to be  $x$ -independent. Eq. (3.14) reduces to the non-linear differential equation using Eqs. (3.4), (3.17) and (3.18):

$$(1 + \varepsilon\theta + Nr)\theta'' + \text{Pr} (f\theta' - (rf' - \beta)\theta) + \varepsilon\theta'^2 = 0, \quad (3.19)$$

where,  $\text{Pr} = \left( \frac{\mu C_p}{k_\infty} \right)$ , is the Prandtl number,  $Nr = \frac{16\sigma^* T_\infty^3}{3k^* k_\infty}$  is the radiation parameter and  $\beta = \frac{\dot{q}}{\mu C_p b}$  is the heat source/sink parameter.

Eqs. (3.15) and (3.16), using Eqs. (3.17) and (3.18) can be written as:

$$\left. \begin{aligned} \theta(0) &= 1 & (PST \text{ Case}) \\ \theta'(0) &= -1 & (PHF \text{ Case}) \end{aligned} \right\}, \quad \theta(\infty) = 0. \quad (3.20)$$

#### 4. ANALYTIC SERIES SOLUTIONS USING HOMOTOPY ANALYSIS METHOD

In general, it is quite difficult to solve highly nonlinear partial differential equations analytically. The much celebrated perturbation technique can be used for this purpose but only for weakly nonlinear problems. In 1992, Liao [26, 27] developed a new analytical technique called the homotopy analysis method (HAM) to tackle such nonlinear problems [28-31]. Being different from perturbation technique, HAM does not need any small parameter. As a matter of fact, the homotopy analysis method can be regarded as a unification of previous non-perturbation techniques such as Adomian method. By its very nature, HAM provides a family of series solutions whose convergence region can be adjusted and controlled by an auxiliary parameter. It is worth mentioning that the homotopy analysis method has successfully been applied to many nonlinear problems in solid and fluid mechanics [32-39]. Having said this, it should be conceded that the number of unsteady nonlinear problems solved using this method is rather limited [35-39].

The first step in the HAM is to find a set of base functions to express the sought solution of the problem under investigation. As mentioned by Liao [31], a solution may be expressed with different base functions, among which some converge to the exact solution of the problem faster than others. Noting that, from the boundary conditions (3.6) and (3.20) and according to rule of solution expression, it is straightforward to choose the initial guesses for  $f(\eta)$  and  $\theta(\eta)$  in the following forms:

$$f_0(\eta) = 1 - \exp(-\eta), \quad (4.1)$$

$$\theta_0(\eta) = \exp(-\eta), \quad \text{for } PST \text{ Case}, \quad (4.2a)$$

$$\theta_0(\eta) = \exp(-\eta), \quad \text{for } PHF \text{ Case}. \quad (4.2b)$$

Furthermore, we choose

$$L_1[f] = f''' - f', \quad (4.3)$$

$$L_2[\theta] = \theta'' + \theta', \quad (4.4)$$

as our auxiliary linear operators, which have the following properties

$$L_1(c_3 \exp(-\eta) + c_2 \eta + c_1) = 0, \quad (4.5)$$

$$L_2(c_4 \exp(-\eta) + c_5) = 0, \quad (4.6)$$

where  $c_i$  ( $i = 1 - 5$ ) are integral constants. Then we construct the so-called *Zereth-order deformation equations*:

$$(1-p)L_1[f(\eta, p) - f_0(\eta)] = p\hbar_1 N_1[f(\eta, p)], \quad (4.7)$$

$$(1-p)L_2[\theta(\eta, p) - \theta_0(\eta)] = p\hbar_2 N_2[f(\eta, p), \theta(\eta, p)], \quad (4.8)$$

subject to the boundary conditions

$$f(0, p) = 0, \quad f'(0, p) = 1, \quad f'(\infty, p) = 0, \quad (4.9)$$

$$\theta(\infty, p) = 0, \quad \begin{cases} \theta(0, p) = 1 & \text{for } PST \text{ Case,} \\ \theta'(0, p) = -1 & \text{for } PHF \text{ Case} \end{cases} \quad (4.10)$$

Under the definitions

$$N_1[f(\eta, p)] = \left( \frac{\partial f(\eta, p)}{\partial \eta} \right)^2 - f(\eta, p) \frac{\partial^2 f(\eta, p)}{\partial \eta^2} - \frac{\partial^3 f(\eta, p)}{\partial \eta^3} + M_n \frac{\partial f(\eta, p)}{\partial \eta} + k_1 \left\{ 2 \frac{\partial f(\eta, p)}{\partial \eta} \frac{\partial^3 f(\eta, p)}{\partial \eta^3} - f(\eta, p) \frac{\partial^4 f(\eta, p)}{\partial \eta^4} - \left( \frac{\partial^2 f(\eta, p)}{\partial \eta^2} \right)^2 \right\}, \quad (4.11)$$

$$N_2[f(\eta, p), \theta(\eta, p)] = (1 + \varepsilon \theta(\eta, p) + Nr) \frac{\partial^2 \theta(\eta, p)}{\partial \theta^2} + Pr \left( f(\eta, p) \frac{\partial \theta(\eta, p)}{\partial \theta} - \left( r \frac{\partial f(\eta, p)}{\partial \eta} - \beta \right) \theta \right) + \varepsilon \left( \frac{\partial \theta(\eta, p)}{\partial \theta} \right)^2, \quad (4.12)$$

where  $p \in [0, 1]$  denotes the embedding parameter,  $\hbar_1$  and  $\hbar_2$  indicates non-zero auxiliary parameters. Obviously, for  $p = 0$  and  $p = 1$ , we have

$$f(\eta, 0) = f_0(\eta), \quad \theta(\eta, 0) = \theta_0(\eta), \quad (4.13)$$

$$f(\eta, 1) = f(\eta), \quad \theta(\eta, 1) = \theta(\eta), \quad (4.14)$$

By Taylor's power series and using equations (4.15) and (4.16),  $f(\eta; p)$  and  $\theta(\eta; p)$  can be expanded in a power series of  $p$  as follows:

$$f(\eta, p) = f(\eta, 0) + \sum_{m=1}^{+\infty} f_m(\eta) p^m, \quad (4.15)$$

$$\theta(\eta, p) = \theta(\eta, 0) + \sum_{m=1}^{+\infty} \theta_m(\eta) p^m, \quad (4.16)$$

where

$$f_m(\eta) = \frac{1}{m!} \left. \frac{\partial^m f(\eta, p)}{\partial p^m} \right|_{p=0}, \quad (4.17)$$

$$\theta_m(\eta) = \frac{1}{m!} \left. \frac{\partial^m \theta(\eta, p)}{\partial p^m} \right|_{p=0}, \quad (4.18)$$

Note that the convergence regions of the series (4.15) and (4.16) are dependent upon the auxiliary parameters  $\hbar_1$  and  $\hbar_2$ . If these auxiliary parameters are properly chosen so that series (4.15) and (4.16) are convergent at  $p = 1$ , therefore using equations (4.13) and (4.14), we have:

$$f(\eta) = f_0(\eta) + \sum_{m=1}^{+\infty} f_m(\eta) p^m, \quad (4.19)$$

$$\theta(\eta) = \theta_0(\eta) + \sum_{m=1}^{+\infty} \theta_m(\eta) p^m, \quad (4.20)$$

Differentiating the Eqs. (4.7)-(4.8)  $m$  times with respect to  $p$  and then setting  $p = 0$  and finally dividing them by  $m!$  we obtain the so-called  $m$ th-order deformation equations for  $f_m(\eta)$  and  $\theta_m(\eta)$  (for details, please refer to Liao [43])

$$L_1[f_m(\eta) - \chi_m f_{m-1}(\eta)] = \hbar_1 R_m^f, \quad (4.21)$$

$$L_2[\theta_m(\eta) - \chi_m \theta_{m-1}(\eta)] = \hbar_2 R_m^\theta, \quad (4.22)$$

subject to the boundary conditions

$$f_m(0) = 0, \quad f'_m(0) = 1, \quad f'_m(\infty) = 0, \quad (4.23)$$

$$\theta_m(\infty) = 0, \quad \begin{cases} \theta_m(0) = 0 & \text{for } PST \text{ Case,} \\ \theta'_m(0) = 0 & \text{for } PHF \text{ Case} \end{cases} \quad (4.24)$$

under the definitions

$$f_m(0) = 0, \quad f'_m(0) = 1, \quad f'_m(\infty) = 0, \quad (4.25)$$

$$\theta_m(\infty) = 0, \quad \begin{cases} \theta_m(0) = 0 & \text{for } PST \text{ Case,} \\ \theta'_m(0) = 0 & \text{for } PHF \text{ Case} \end{cases} \quad (4.26)$$

and

$$\chi_m = \begin{cases} 0, & m \leq 1, \\ 1, & m > 1. \end{cases} \quad (4.27)$$

$$f(\eta) = f_0(\eta) + \sum_{m=1}^{+\infty} f_m(\eta) p^m, \quad (4.28)$$

$$\theta(\eta) = \theta_0(\eta) + \sum_{m=1}^{+\infty} \theta_m(\eta) p^m. \quad (4.29)$$

### 5. RESULTS AND DISCUSSION

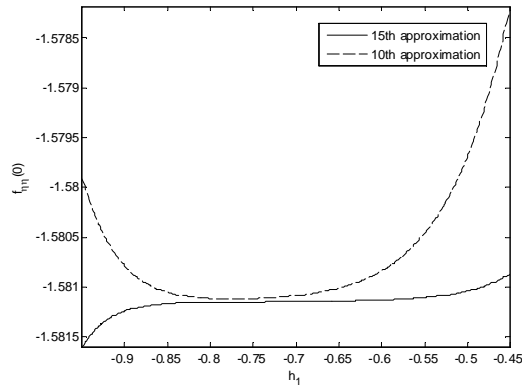
As proved by Liao [31], as long as the series solutions (Eq. (4.28) and Eq. (4.29)) are convergent, they should converge to one of the solutions of Eq. (3.5) and Eq. (3.19). Note that the Eqs. (4.28) and (4.29) contain auxiliary parameters  $\hbar_1$  and  $\hbar_2$  which are not yet defined. These parameters play an important role in the framework of HAM. In fact, these parameters control the rate of convergence and the convergence region of the series. Proper values for these auxiliary parameters can be found by plotting the so-called  $\hbar$ -curves. When the valid region of  $\hbar$  is a horizontal line segment then the solution is converged. Figure 2 shows the  $\hbar_1$ -curve and Figs. 3 and 4 show typical  $\hbar_2$ -curves for both PST and PHF cases for a given set of parameters,  $k_1 = 0.2$ ,  $Mn = 1$ ,  $Pr = 1$ ,  $\beta = 0$ ,  $\varepsilon = 0$ ,  $r = 2$ ,  $Nr = 0$ . A wide valid zone is evident in these figures ensuring convergence of the series for both PST and PHF cases. Having chosen the best values for  $\hbar$ , we are able to present the velocity profiles obtained for different combinations of  $k_1$  and  $Mn$ , and investigate the effects of different parameters such as visco-elastic parameter, Radiation parameter, magnetic number, Prandtl number, wall temperature parameter, and heat source/sink parameter on the temperature field above the sheet for both PST and PHF cases. The obtained analytical results are illustrated in Figs. 5-19 and Table 1-2.

**Table 1**  
The Best Values of the Auxiliary Parameters and Wall Temperature Gradients for the PST Case

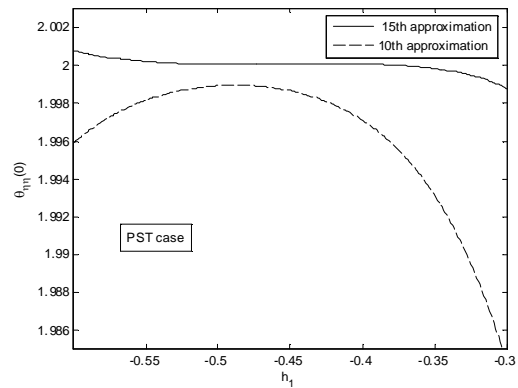
$k_1$	Pr	$\beta$	$\varepsilon$	$r$	$Nr$	$Mn$	$\hbar_1$	$\hbar_2$	$\theta_1(0)$
0	1.0	0.0	0.0	2.0	0.0	1.0	-0.69	-0.47	-1.21550
0.2	1.0	0.0	0.0	2.0	0.0	1.0	-0.71	-0.44	-1.16859
0.4	1.0	0.0	0.0	2.0	0.0	1.0	-0.72	-0.53	-1.10125
0.1	1.0	-0.1	0.0	2.0	0.0	0.1	-0.98	-0.58	-1.35219
0.1	1.0	0.0	0.0	2.0	0.0	0.1	-0.98	-0.62	-1.30354
0.1	1.0	0.1	0.0	2.0	0.0	0.1	-0.98	-0.67	-1.24954
0.1	1.0	-0.1	0.0	2.0	1.0	0.1	-0.98	-0.5	-0.87594
0.1	1.0	-0.1	0.0	2.0	3.0	0.1	-0.98	-0.23	-0.54886
0.1	1.0	-1.0	0.0	0.0	0.0	0.1	-0.98	-0.82	-0.65243
0.1	1.0	-1.0	0.0	-2.0	0.0	0.1	-0.98	-1	-0.58039
0.2	1.0	0.0	0.0	2.0	0.0	0.0	-1.08	-0.64	-1.3000
0.2	1.0	0.0	0.0	2.0	0.0	2.0	-0.5	-0.51	-1.07009
0.2	1.0	-0.1	0.0	2.0	0.0	1.0	-0.71	-0.44	-1.23432
0.2	2.0	-0.1	0.0	2.0	0.0	1.0	-0.71	-0.3	-1.89600
0.2	3.0	-0.1	0.0	2.0	0.0	1.0	-0.71	-0.2	-2.29220

**Table 2**  
The Best Values of the Auxiliary Parameters and Wall Temperature  $\theta(0)$  for the PHF Case

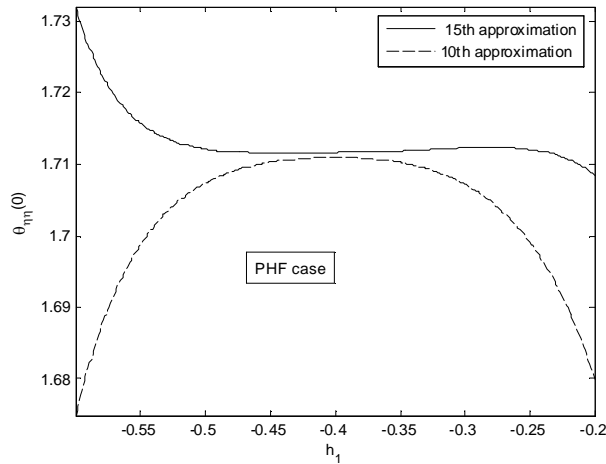
$k_1$	Pr	$\beta$	$\varepsilon$	$r$	$Nr$	$Mn$	$\tilde{h}_1$	$\tilde{h}_2$	$\theta(0)$
0	1.0	-0.1	0.0	2.0	0.0	1.0	-0.69	-0.4	0.78601
0.2	1.0	-0.1	0.0	2.0	0.0	1.0	-0.71	-0.37	0.81025
0.4	1.0	-0.1	0.0	2.0	0.0	1.0	-0.72	-0.46	0.97915
0.1	1.0	-0.1	0.0	2.0	0.0	0.1	-0.98	-0.44	0.73953
0.1	1.0	0.0	0.0	2.0	0.0	0.1	-0.98	-0.48	0.76712
0.1	1.0	0.1	0.0	2.0	0.0	0.1	-0.98	-0.52	0.80024
0.1	1.0	-0.1	0.0	2.0	1.0	0.1	-0.98	-0.48	1.14161
0.1	1.0	-0.1	0.0	2.0	3.0	0.1	-0.98	-0.3	1.82175
0.1	1.0	-0.1	0.0	0.0	0.0	0.1	-0.98	-0.98	1.53271
0.2	1.0	-0.1	0.0	2.0	0.0	0.0	-1.08	-0.42	0.74127
0.2	1.0	-0.1	0.0	2.0	0.0	2.0	-0.5	-0.41	0.87655
0.2	1.0	-0.1	0.0	2.0	0.0	1.0	-0.71	-0.37	0.81025
0.2	2.0	-0.1	0.0	2.0	0.0	1.0	-0.71	-0.19	0.52466
0.2	3.0	-0.1	0.0	2.0	0.0	1.0	-0.71	-0.13	0.42053



**Figure 2:** Typical  $\tilde{h}_1$ -Curve for  $k_1 = 0.2$

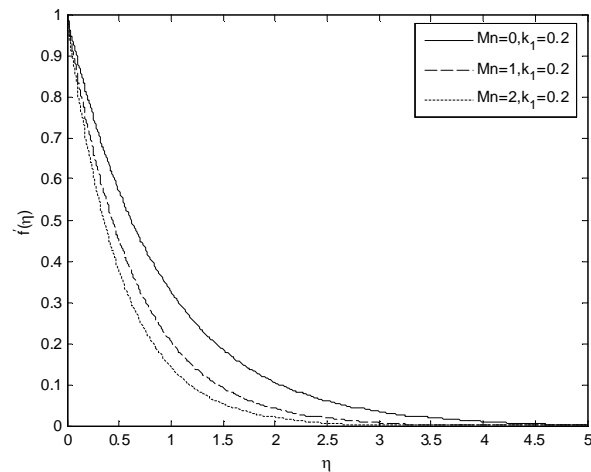


**Figure 3:** Typical  $\tilde{h}_2$ -Curves for  $k_1 = 0.2$ ,  $Mn = 1$ ,  $Pr = 1$ ,  $\beta = 0$ ,  $\varepsilon = 0$ ,  $r = 2$ ,  $Nr = 0$ ,  $h_1 = -0.71$  for PST Case



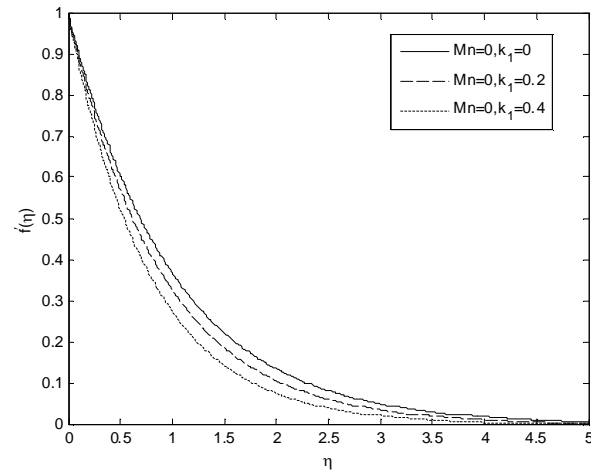
**Figure 4:** Typical  $h_2$ -Curves for  $k_1 = 0.2$ ,  $Mn = 1$ ,  $Pr = 1$ ,  $\beta = 0$ ,  $\varepsilon = 0$ ,  $r = 2$ ,  $Nr = 0$ ,  $h_1 = -0.71$  for PHF Case

Figure 5 is a graphical representation which depicts the effect of magnetic field parameter  $Mn$  on the horizontal velocity profile  $f_\eta(\eta)$ . It is found that the effect of magnetic field parameter  $Mn$  is to reduce the horizontal velocity profile  $f_\eta(\eta)$ . This graphical representation reveals that magnetic field parameter  $Mn$  decreases the horizontal velocity profile  $f_\eta(\eta)$ , significantly in the visco-elastic flow in comparison with the viscous flow, this is due to the fact that increase of  $Mn$  signifies the increase of Lorentz force, which opposes the horizontal flow in the reverse direction.



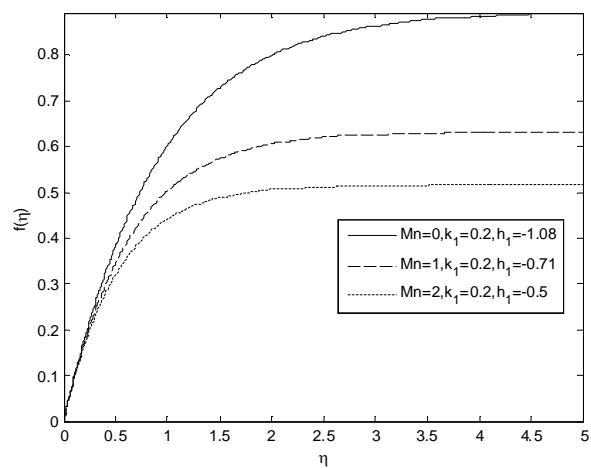
**Figure 5:** Effect of Magnetic Parameter  $Mn$  on Horizontal Velocity

Figure 6 shows the effect of visco-elastic parameter,  $k_1$  on the horizontal velocity profile  $f_\eta(\eta)$ . The effect of visco-elastic parameter  $k_1$  is seen to decrease the boundary layer velocity throughout the boundary layer but significantly near the stretching sheet.



**Figure 6:** Effect of Visco-Elastic Parameter  $k_1$  on Horizontal Velocity

Figure 7-8 represents variations in the transverse velocity for different numerical values of visco-elastic parameter  $k_1$  and magnetic parameter  $Mn$ . Obviously transverse velocity  $v$  is enhanced as visco-elastic parameter  $k_1$  or magnetic parameter  $Mn$  rises. Idrees and Abel [40] have shown that visco-elasticity acts physically to increase the adherence to the wall of the hydrodynamic boundary layer, which in turn retards the flow in the horizontal direction explaining the monotonically decreasing nature of the curves. The drag force appears as a term  $M_n f'$  in the transform momentum of Eq. (3.5) and serves to retire the momentum in the positive direction of the  $x$ -axis, also affecting via the coupling with the other terms, the momentum in the  $y$ -direction. The shear stresses are therefore lowered at the wall as  $Mn$  is increased, which decreases both  $u$  and  $v$  velocities. In both cases the maximum values of shear stress are reported at  $\eta = 0$ .



**Figure 7:** Effect of Magnetic Parameter  $Mn$  on Transverse Velocity

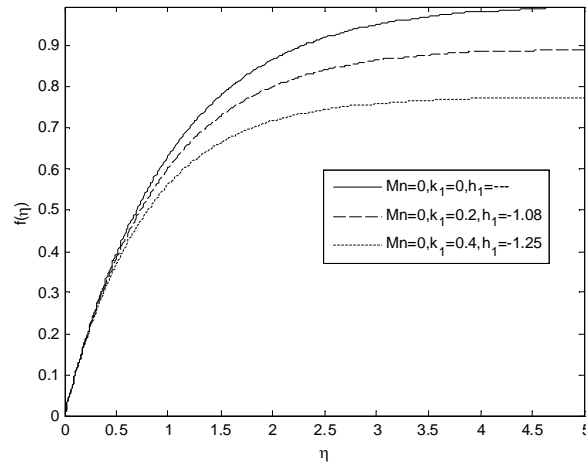


**Figure 8:** Effect of Visco-Elastic Parameter  $k_1$  on Transverse Velocity

These findings of the study correlate very well with the general conclusions arrived at by other classical magnetohydrodynamic studies including those of Cramer and Pai [41], Siddheshwar and Mahabaleshwar [42]. It is noted that the depression in the horizontal velocity is less prominent than the transverse velocity. Thus the influence of magnetic field is to aid more strongly in decelerating the flow perpendicular to the plate.

Figures 9-10 demonstrate the effect of visco-elastic parameter " $k_1$ " on the temperature profile  $\theta(\eta)$  in the boundary layer in PST and PHF cases respectively. It is observed that the temperature profile decreases in the boundary layer with the increase of distance from the boundary. It is also noticed that the temperature distribution is unchanged at the wall with the change of physical parameters. However, it tends to zero in the free stream. The temperature increases with the increasing values of visco-elastic parameter  $k_1$  both in the case of PST and PHF. This is due to

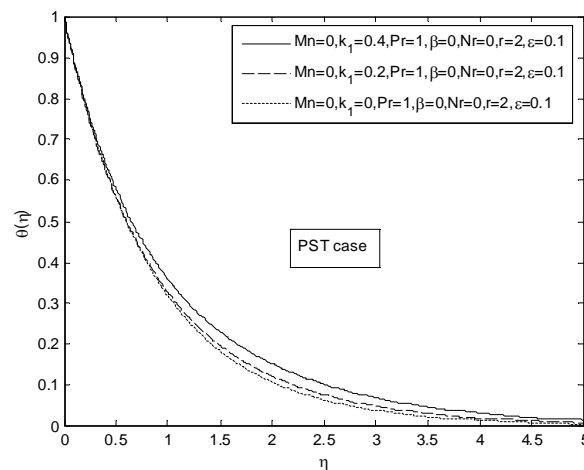


**Figure 9:** Effect of Visco-Elastic Parameter  $k_1$  on the Temperature Profile in  $\theta(\eta)$  PHF case

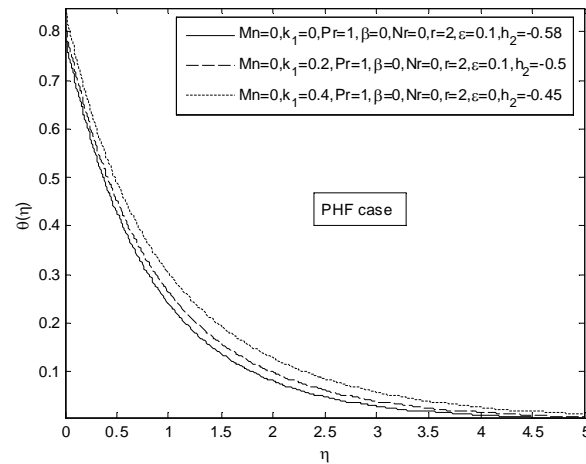


**Figure 10:** Effect of Visco-Elastic Parameter  $k_1$  on the Temperature Profile in  $\theta(\eta)$  PHF Case

the fact that the thickening of thermal boundary layer occurs due to the increase of visco-elastic normal stress. From Tables 1 and 2, we observe that the effect of visco-elastic parameter is to increase the wall temperature gradient  $-\theta'_\eta(0)$  in PST case and the wall temperature  $\theta(0)$  in PHF case.

The effect of magnetic parameter  $Mn$  on temperature profile  $\theta(\eta)$  in the presence/absence of variable thermal conductivity is shown in Figs. 11-12 in case of PST and PHF respectively. It is noticed that the effect of magnetic parameter is to increase the temperature profile  $\theta(\eta)$  in the boundary layer. This is because of the fact that the introduction of transverse magnetic field to an electrically conducting fluid gives rise to a body force known as Lorentz force which opposes the motion. The resistance offered to the flow because of this force is responsible in enhancing the temperature. Also, the effect on the flow and thermal fields become more so as

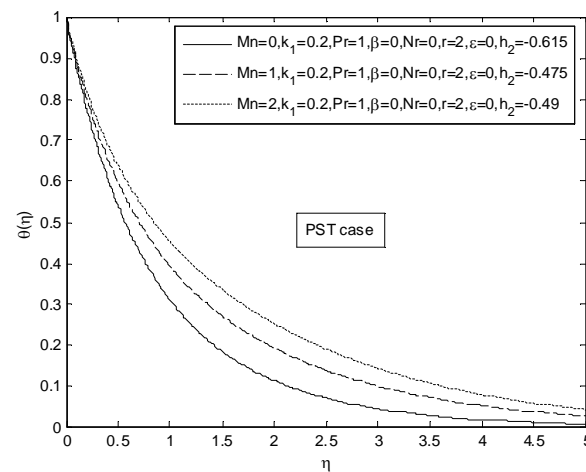


**Figure 11:** Effect of Magnetic Parameter  $Mn$  on Temperature Profile in  $\theta(\eta)$  PST Case

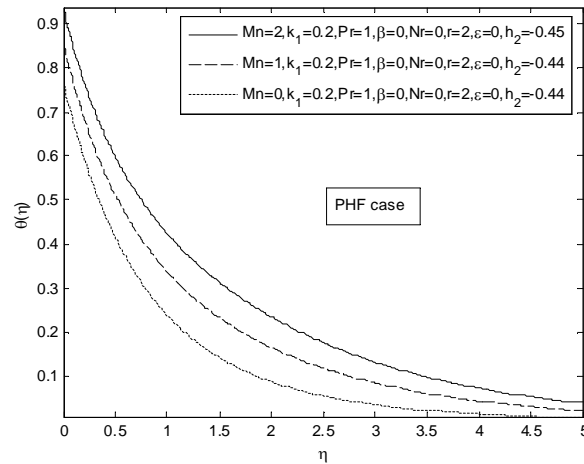


**Figure 12:** Effect of Magnetic Parameter  $Mn$  on Temperature Profile  $\theta(\eta)$  in PHF Case

the strength of the magnetic field increases. The effect of magnetic parameter  $Mn$  is to increase the wall temperature gradient  $-\theta'_{\eta}(0)$  in PST case and the wall temperature  $\theta(0)$  in PHF case. This is due to the fact that thermal boundary layer thickness decreases as the magnetic parameter  $Mn$  increases which results in higher temperature gradient at the wall and hence higher heat transfer at the wall.

For fixed values of Prandtl number and magnetic parameter the effect of wall temperature parameter  $r$ , on the temperature profile  $\theta(\eta)$  in the boundary layer is shown in Figs. 13-14. From the graphical representation we observe that the increase in wall temperature parameter  $r$  leads the temperature profile  $\theta(\eta)$  to decrease and the magnitude of wall temperature gradient increases with wall temperature. This is due to the fact that, when  $r > 0$ , heat flows from the stretching sheet into the ambient medium and, when  $r < 0$ , the temperature gradient is positive and heat flows into the stretching sheet from the ambient medium.

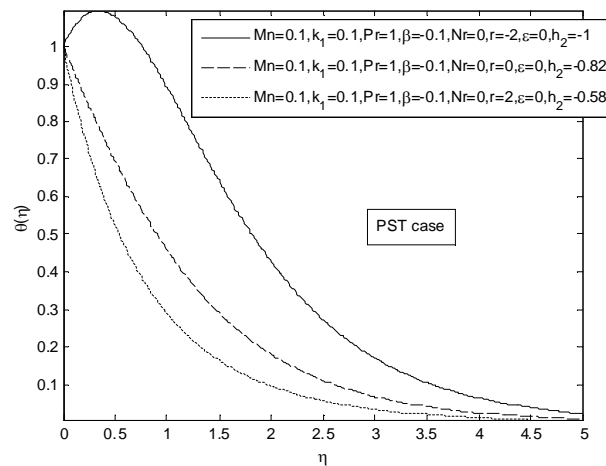


**Figure 13:** Effect of Wall Temperature Parameter  $r$ , on the Temperature Profile  $\theta(\eta)$  in PST Case

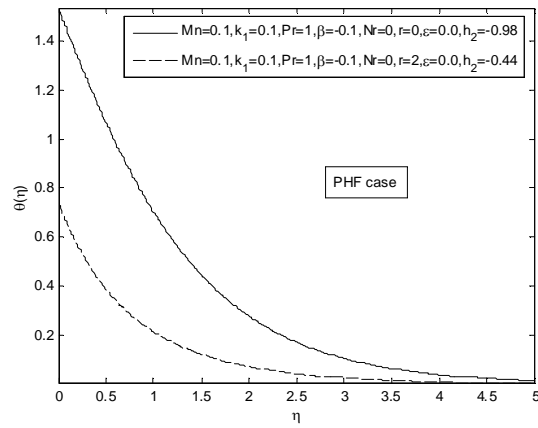


Figure 14(a): Effect of Wall Temperature Parameter  $r$ , on the Temperature Profile  $\theta(\eta)$  in PHF Case

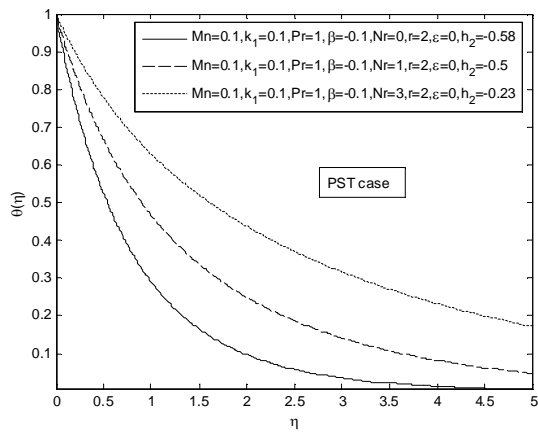


Figure 14(b): Effect of Thermal Radiation on Temperature Profile  $\theta(\eta)$  in PST Case

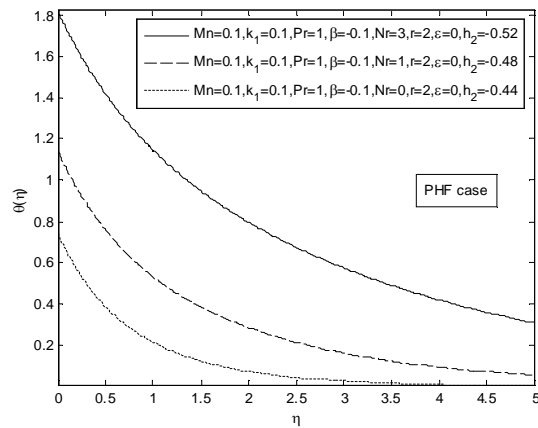


Figure 15: Effect of Thermal radiation on temperature profile  $\theta(\eta)$  in PHF Case

Figures 14-15 shows the effect of thermal radiation on temperature profile  $\theta(\eta)$  in the boundary layer. It is observed that the increase in thermal radiation parameter  $Nr$  produces a significant increase in the thickness of the thermal boundary layer of the fluid and so the temperature profiles  $\theta(\eta)$  increases. The wall gradients of PST and PHF cases increase as the thermal radiation parameter increases which can be observed in Tables 1 and 2.

The effect of heat source/sink parameter  $\beta$  on temperature profile  $\theta(\eta)$  in the boundary layer is shown in Fig. 5. It is observed that the effect of heat source  $\beta > 0$  in the boundary layer generates the energy which causes the temperature to increase, while the presence of heat sink  $\beta < 0$  in the boundary layer absorbs the energy which causes the temperature to decrease. These behaviours are seen in Fig. 5. From Tables 1 and 2 we see that the effect of heat source is more pronounced as compared to that of heat sink. These behaviours are even true in the presence of variable thermal conductivity.

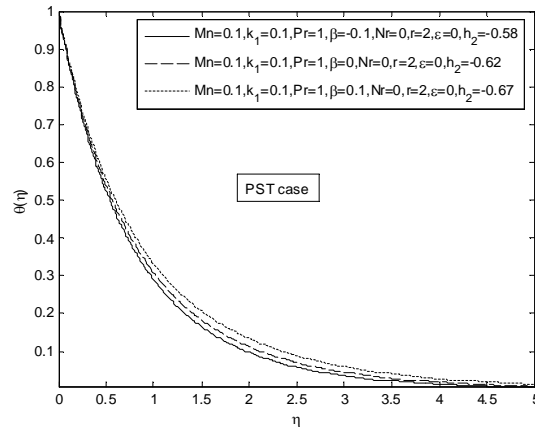


Figure 16: Effect of Heat Source/Sink Parameter  $\beta$  on Temperature Profile in PST Case

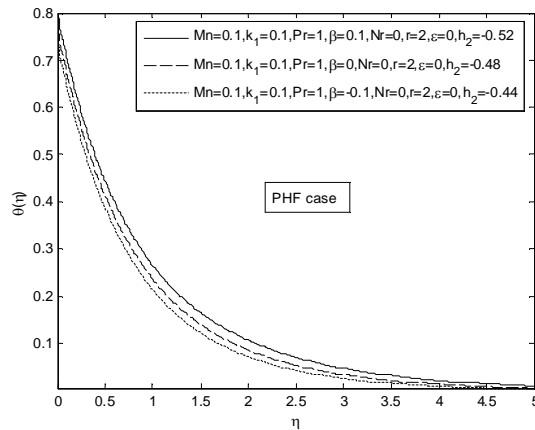


Figure 17: Effect of Heat Source/Sink Parameter  $\beta$  on Temperature Profile in PST Case

Fig. 6 demonstrates the effect of Prandtl number on temperature profile in the boundary layer. It is seen that the effect of Prandtl number is to decrease the temperature profile in the boundary layer. This is because of the fact that thermal boundary thickness decreases with increase in Prandtl number. It is also observed from Tables 1 and 2 that the heat transfer increases with Prandtl number because a higher Prandtl number fluid has relatively lower thermal conductivity which reduces conduction and there by increases the variation. This results in the reduction of the thermal boundary layer thickness and increase in the heat transfer at the wall. For PHF case, the temperature at the wall reduces as the Prandtl number increases because of the cooling effect on the surface caused by the increase in Prandtl number.

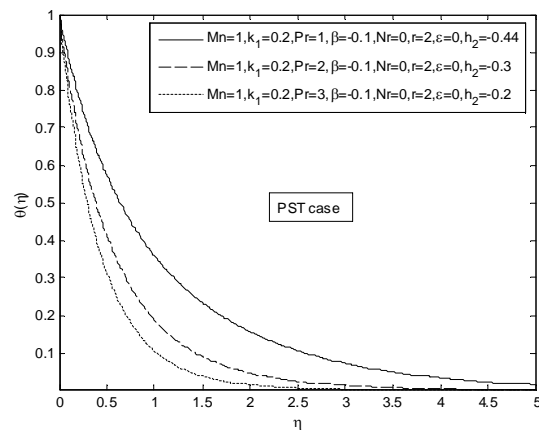


Figure 18: Effect of Prandtl Number on Temperature Profile in PST Case

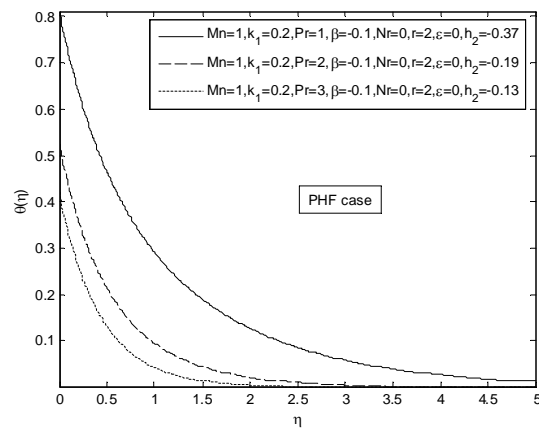


Figure 19: Effect of Prandtl Number on Temperature Profile in PHF Case

## REFERENCES

- [1] Crane L. J., Flow Past a Stretching Plate, *Z Angew Math. Phys.*, 21, (1970), 645-647.
- [2] Gupta P. S., and Gupta A. S., Heat and Mass Transfer on a Stretching Sheet with Suction or Blowing, *Can J. Chem Eng.*, 55, (1977), 744-746.

- [3] Chen C. K., and Char M. I., Heat Transfer of a Continuous Stretching Surface with Suction or Blowing, *J. Math. Anal. Appl.*, 135, (1988), 568-580.
- [4] Datta B. K., Roy P., and Gupta A. S., Temperature Field in the Flow Over a Stretching Sheet with Uniform Heat Flux, *Int. Comm. Heat Mass Transfer*, 12, (1985), 89-94.
- [5] McLeod B., and Rajagopal K. R., On the Non-Uniqueness of the Flow of a Navier-Stokes Fluid Due to Stretching Boundary, *Arch Ration Mech. Anal.*, 98, (1987), 385-493.
- [6] Chiam T. C., Heat Transfer with Variable Thermal Conductivity in a Stagnation Point Towards a Stretching Sheet, *Int. Comm. Heat Mass Transfer*, 23(2), (1996), 239-248.
- [7] Chiam T. C., Heat Transfer in a Fluid with Variable Thermal Conductivity Over a Linearly Stretching Sheet, *Acta Mech.*, 129, (1998), 63-72.
- [8] Rajagopal K. R., Na T. Y., and Gupta A. S., Flow of a Visco-Elastic Fluid Over a Stretching Sheet, *Rheol Acta*, 23, (1984), 213-215.
- [9] Siddappa B., Abel M. S., Non-Newtonian Flow Past a Stretching Plate, *Z Angew Math Phys.*, 36, (1985), 47-54.
- [10] Troy W. C., Overmann II E. A., Eremont-Rout G. B., and Keener J. P., Uniqueness of the Flow of Second Order Fluid Flow Past a Stretching Sheet. *Quart. Appl. Math.*, 44, (1987), 753-755.
- [11] Wen-Dong Chang. The Non-Uniqueness of the Flow of a Visco-Elastic Fluid Over a Stretching Sheet, *Quart. Appl. Math.*, 47, (1989), 365-366.
- [12] Sam Lawrence P., and Nageswara Rao B., The Non-Uniqueness of the MHD Flow of a Visco-Elastic Fluid Past a Stretching Sheet, *Acta Mech.*, 112, (1995), 223-225.
- [13] Abel M. S., and Veena P. H., Visco-Elastic Fluid Flow and Heat Transfer in a Porous Medium Over a Stretching Sheet, *Int. J. non-Linear Mech.*, 33, (1998), 531-538.
- [14] Bujurke N. M., Biradar S. N., and Hiremath P. S., Second Order Fluid Flow Past a Stretching Sheet with Heat Transfer, *Z Angew Math Phys.*, (ZAMP), 38, (1987), 653-657.
- [15] Prasad K. V., Subhas Abel, and Khan S. K., Momentum and Heat Transfer in a Visco-Elastic Fluid Flow in a Porous Medium Over a Non-Isothermal Stretching Sheet, *Int. J. Numer Meth. Heat Fluid Flow*, 10(8), (2000), 786-801.
- [16] Prasad K. V., Subhas Abel M., and Datti P. S., Diffusion of Chemically Reactive Species of a Non-Newtonian Fluid Immersed in a Porous Medium Over a Stretching Sheet, *Int. J. Non-Linear Mech.*, 38(5), (2003), 651-657.
- [17] Sarpakaya T., Flow on Non-Newtonian Fluids in a Magnetic Field, *Amm. Inst. Chem. Ing. J.*, 7, (1961), 26-28.
- [18] Pavlov K. B., Magneto-Hydrodynamic Flow of an Incompressible Viscous Fluid Caused by Deformation of a Plane Surface, *Magninaya Gidrodinamika (USSR)*, 4, (1974), 146-147.
- [19] Chakrabarti A., and Gupta A. S., Hydro-Magnetic Flow and Heat Transfer Over a Stretching Sheet, *Quart. Appl. Math.*, 37, (1979), 73-8.
- [20] Char M. I., Heat and Mass Transfer in a Hydro-Magnetic Flow of a Visco-Elastic Fluid Over a Stretching Sheet, *J Math. Anal. Appl.*, 186, (1994), 674-689.
- [21] Andersson H. I., MHD Flow of a Visco-Elastic Fluid Past a Stretching Surface, *Acta Mech.*, 95, (1992), 227-230.
- [22] Datti P. S., Prasad K. V., Subhas Abel M., and Ambuja Joshi, MHD Fluid Flow Over a Non-Isothermal Stretching Sheet, *Int. J. Engg. Sci.*, 42, (2004), 935-946.
- [23] Beard D. W., and Walters K., Elastic-Viscous Boundary Layer Flows, Two-Dimensional Flow Near a Stagnation Point, *Proc Cambr Phil Soc.*, 60, (1964), 667-674.
- [24] Chiam T. C., Magneto-hydrodynamic Heat Transfer Over a Non-Isothermal Stretching Sheet, *Acta Mech.*, 122, (1997), 169-179.
- [25] M. Quinn Brewster, *Thermal Radiative Transfer Properties*, John Wiley and Sons, New York, (1992).
- [26] Hilton P. J., *An Introduction to Homotopy Theory*, Cambridge University Press, (1953).
- [27] Liao S. J., *The Proposed Homotopy Analysis Techniques for the Solution of Nonlinear Problems*, *Ph.D Dissertation*, Shanghai: Shanghai Jiao Tong University, (1992), [In English].

- [28] Liao S. J., A Second-Order Approximate Analytical Solution of a Simple Pendulum by the Process Analysis Method. *J. Appl. Mech. Trans. ASME*, 59, (1992), 970.
- [29] Liao S. J., A Kind of Approximate Solution Technique which Does not Depend Upon Small Parameters (II): An Application in Fluid Mechanics, *Int. J. Non-Linear Mech.*, 32, (1997), 815.
- [30] Liao S. J., An Explicit Totally Analytic Approximation of Blasius Viscous Flow Problems, *Int. J. Non-linear Mech.*, 34, (1999), 759.
- [31] Liao S. J., *Beyond Perturbation: Introduction to Homotopy Analysis Method*, Boca Raton, Chapman & Hall/CRC Press, (2003).
- [32] Liao S. J., A Uniformly Valid Analytic Solution of Two-Dimensional Viscous Flow Over a Semi-Infinite Flat Plate, *J Fluid Mech.*, 385, (1999), 101.
- [33] Liao S. J, and Campo A., Analytic Solutions of the Temperature Distribution in Blasius Viscous Flow Problems, *J. Fluid Mech.*, 453, (2002), 411.
- [34] Liao S. J., On the Analytic Solution of Magneto-hydrodynamic Flows of Non-Newtonian Fluids Over a Stretching Sheet, *J. Fluid Mech.*, 488, (2003), 189.
- [35] Liao S. J., An Analytic Solution of Unsteady Boundary-Layer Flows Caused by an Impulsively Stretching Plate, *CNSNS*, 11, (2006), 326.
- [36] Xu H, Liao S. J., and Pop I., Series Solutions of Unsteady Three-Dimensional MHD Flow and Heat Transfer in the Boundary Layer Over an Impulsively Stretching Plate, *Euro J. Mech. B, Fluids*, 26, (2007), 15.
- [37] Xu H., Liao S. J. Series Solutions of Unsteady Magneto-hydrodynamic Flows of Non-Newtonian Fluids Caused by an Impulsively Stretching Plate. *J. Non-Newton Fluid Mech.*, 159, (2005), 46.
- [38] Cheng J., Liao S. J., and Pop I., Analytic Series Solution for Unsteady Mixed Convection Boundary Layer Flow Near the Stagnation Point on a Vertical Surface in a Porous Medium, *Trans Porous Med.*, 61, (2005), 365.
- [39] Abbas Z., Hayat T., Sajid M., and Asghar S., Unsteady Flow of a Second Grade Fluid Film Over an Unsteady Stretching Sheet, *Math Comput Model.*, doi:10.1016/j.mcm.2007.09.015.
- [40] M. K. Idrees, and M. S. Abel, Visco-Elastic Flow Past a Stretching Sheet in Porous Media and Heat Transfer with Internal Heat Source, *Indian J. Theor. Phys.*, 44, (1996), 233-244.
- [41] K. R. Cramer, and S. I. Pai, Magneto-Fluid Dynamics for Engineers and Applied, *Physicists*, McGraw-Hill, NewYork, (1973).
- [42] P. G. Siddheshwar, and U. S. Mahabaleshwar, Effects of Radiation and Heat Source on MHD Flow of a Visco-Elastic Liquid and Heat Transfer Over a Stretching Sheet, *Int. J. Non-Linear Mech.*, 40, (2005), 807-821.
- [43] Liao S. J., and Tan Y. A., General Approach to Obtain Series Solutions of Nonlinear Differential Equations, *Stud. Appl. Math.*, 119, (2007), 297.